Theor Chem Acc (2003) 110:28–33
DOI 10.1007/s00214-003-0449-z

Theoretical
Chemistry Accounts

Regular article

Valence ab initio calculation of the potential-energy curves for the Ca_2 dimer

E. Czuchaj[1], **M. Krośnicki**[1], **H. Stoll**[2]

[1] Institute of Theoretical Physics and Astrophysics, University of Gdańsk, ul. Wita Stwosza 57, 80-952 Gdańsk, Poland
[2] Institut für Theoretische Chemie, Universität Stuttgart, Pfaffenwaldring 55, 70550 Stuttgart, Germany

Received: 13 February 2003 / Accepted: 3 April 2003 / Published online: 16 July 2003

Abstract. The electronic structure of the Ca_2 molecule has been investigated by use of a two-valence-electron semiempirical pseudopotential and applying the internally contracted multireference configuration interaction method with complete-active-space self-consistent-field reference wave functions. Core–valence correlation effects have been accounted for by adding a core-polarization potential to the Hamiltonian. The ground-state properties of the Ca_2 and Ca_2^+ dimers have also been studied at the single-reference coupled-cluster level with single and double excitations including a perturbative treatment of triple excitations. Good agreement with experiment has been obtained for the ground-state potential curve and the only experimentally known $A^1\Sigma_u^+$ excited state of Ca_2. The spectroscopic parameters D_e and R_e deduced from the calculated potential curves for other states are also reported. In addition, spin–orbit coupling between the singlet and triplet molecular states correlating, respectively, with the $(4p)^1P$ and $(4p)^3P$ Ca terms has been investigated using a semi-empirical two-electron spin–orbit pseudopotential.

Keywords: Collision complexes – Dimers – Potential curves – Transition moments

1 Introduction

The alkaline-earth dimers are of interest because of their weakly bound ground states at large internuclear distances and more strongly bound excited states. This causes spectral transitions between the excited states and the ground state to appear as broad continua that are shifted far to the red from the corresponding atomic lines. Transitions of this type are very well suited for laser applications. Moreover, the major isotopes of alkaline-earth atoms have no nuclear spin and thus lack hyperfine structure. Owing to that, these species have become of interest because of the possibility of using them in studies of cold collisions of atoms. Cold collisions offer, among others, the prospects of quantitative experiments and theory on small-detuning trap loss, high-resolution photoassociation spectroscopy on several molecular states and optical shielding experiments. So far light-induced collisions of cold, neutral alkaline-earth atoms in magnetooptical trap (MOT) experiments have been successfully studied both experimentally and theoretically in many laboratories. The molecular structure involving low-lying states of the alkaline-earth dimers can, in general, be deduced from spectroscopic studies. The potential curves for low-lying states of group IIA dimers were first calculated by Jones [1] using the local spin-density functional formalism. Apart from that, a few other calculations on Mg_2 [2, 3, 4], Ca_2 [5], Sr_2 [6] and Ba_2 [7] were reported in the literature. The available potential curves are, however, still insufficient to yield satisfactory interpretation of experimental results and to test more realistic theories; therefore new ab initio potential curves for these species are greatly desired.

This paper is devoted to the Ca_2 dimer and is a continuation of our earlier studies on alkaline-earth species [4]. Spectroscopical investigations on Ca_2 were conducted, among others, by Bolfour and Whitlock [8], Sakurai and Broida [9], Wyss [10], Miller et al. [11], Vidal [12], Vigue [13], Hofmann and Harris [14] and Gondal et al. [15]. Photoassociation spectroscopy in the Ca MOT experiment was first reported by Zinner et al. [16] and was subsequently studied theoretically by Machholm et al. [17]. The ground state of Ca_2 was investigated teoretically by Dyall and McLean [5], but low-lying excited states were calculated by Jones [1]. The goal of the present study is to calculate the potential energies for the ground state and low-lying excited triplet and singlet states of Ca_2 in a four-valence-electron approach. Hereby, the atomic core was replaced by a semiempirical two-electron pseudopotential [PP(2)]. The core polarization as well as core–valence correlation

Correspondence to: E. Czuchaj
e-mail: czu@iftia.univ.gda.pl

were accounted for by a core polarization potential (CPP) added to the Hamiltonian. The calculations involve the Ca_2 states arising from the $(4s^2)^1S + {}^1S$, $(4s4p)^3P + {}^1S$, $(4s3d)^3D + {}^1S$, $(4s3d)^1D + {}^1S$ and $(4s4p)^1P + {}^1S$ atomic asymptotes and were carried out using the internally contracted multireference configuration interaction method (ICMRCI) with complete-active-space self-consistent-field (CASSCF) reference wave functions. The ground-state potential curves for Ca_2 and Ca_2^+ were also studied at the single-reference coupled-cluster level with single and double excitations including a perturbative treatment of triple excitations [CCSD(T)]. In addition, the spin–orbit (SO) coupling between the excited singlet and triplet molecular states correlating, respectively, with the $(4p)^1P$ and $(4p)^3P$ Ca terms was evaluated at the CASSCF level using a semiempirical SO two-electron pseudopotential. The study of SO coupling is of importance because it provides the basic magnitude of the fine-structure changing mechanism for trap loss rates observed in MOT experiments. All calculations reported in this paper were performed by means of the MOLPRO program package [18]. A brief presentation of the calculational details is given in Sect. 2. The results are discussed in the context of available experimental data in Sect. 3.

2 Computational details

In the present calculations the Ca atom is considered as a two-electron system. That means that only the valence electrons of Ca are treated explicitly, while the Ca core is represented by the semiempirical energy adjusted pseudopotential, V_{ecp} in the form

$$V_{\mathrm{ecp}} = \sum_{i=1}^{N}\left(-\frac{Q}{r_i} + \sum_l B_l \exp(-\beta_l r_i^2)P_l\right), \tag{2}$$

where $Q = 2$ denotes the net charge of the Ca core, P_l is the projection operator onto the Hilbert subspace of angular symmetry l with respect to the Ca^{2+} core and N is the number of valence electrons. In order to account for the core-polarization and core-valence correlation effects, the CPP in the form proposed by Müller et al. [19] was added to the Hamiltonian. The pseudopotential parameters B_l and β_l for Ca, as well as the Ca^{2+} core dipole polarizability (3.06 au) and the cutoff parameter ($0.43\,a_0^{-2}$) defining the polarization potential are taken from Ref. [20]. On the other hand, the SO operator is put in the form

$$V_{\mathrm{so}} = \sum_{l,i}\frac{2\Delta V_{i,l}}{2l+1}P_l\mathbf{l}_i\mathbf{s}_iP_l, \tag{3}$$

where the difference $\Delta V_{i,l}$ of the radial parts of the two-component quasirelativistic pseudopotentials $V_{l,l+1/2}$ and $V_{l,l-1/2}$ is expressed in terms of Gaussian functions

$$\Delta V_{i,l} = \sum_k \Delta A_{lk}\exp(-a_{lk}r_i^2). \tag{4}$$

The coefficients $2\Delta A_l/(2l+1)$ and a_l ($k = 1$) defining the SO operator were determined by Figgen (private communication). They were adjusted to experimental SO splittings of the lowest ^2D and ^2P terms of the singly positive Ca ion. Their numerical values are, respectively, 0.070141 and 0.548 for the P term and 0.001228 and 1.119 for the D term. The contracted (9s7p6d)/[7s6p6d] basis set for Ca optimized in our earlier calculations [21] was augmented by three sets of f polarization functions (exponents 0.264, 0.155, 0.091) and g function (0.166635). The quality of the basis set was examined in configuration interaction calculations for the ground state and several excited states of the Ca atom. For that purpose, the SO-averaged atomic energies were calculated in the *LS* coupling scheme by means of the CASSCF/ICMRCI method. The calculated Ca excitation energies from the $(4s^2)^1S$ ground state to the excited $(4s3p)^3P$, $(4s3d)^3D$, $(4s3d)^1D$ and $(4s4p)^1P$ states are 15121 (15263), 20620 (20356), 21965 (21849) and 23434 (23652) cm^{-1}, respectively. The numbers in parentheses stand for the experimental values [22]. In turn, the evaluated fine-structure splittings are $\Delta E(^3P_1 - {}^3P_0) = 51.3$ ($52.6\ \mathrm{cm}^{-1}$), $\Delta E(^3P_2 - {}^3P_1) = 104.3$ ($105.88\ \mathrm{cm}^{-1}$), $\Delta E(^3D_2 - {}^3D_1) = 16.8$ ($13.9\ \mathrm{cm}^{-1}$) and $\Delta E(^3D_3 - {}^3D_2) = 25.8$ ($21.74\ \mathrm{cm}^{-1}$ [22]). The potential curves for Ca_2 were calculated in the ΛS coupling scheme using the CASSCF method to generate the orbitals for the subsequent cofiguration interaction calculations. The corresponding active space in the D_{2h} point group involved the molecular counterparts of the 4*s*, 3*d* and 4*p* valence orbitals of the Ca atom. Among the 16 molecular orbitals ($6\sigma_g$, $6\sigma_u$, $7\sigma_g$, $7\sigma_u$, $8\sigma_g$, $8\sigma_u$, $9\sigma_g$, $9\sigma_u$, $3\pi_g$, $3\pi_u$, $4\pi_g$, $4\pi_u$; orbitals $2\delta_g$ and $2\delta_u$ of the point group D_{2h} had to be dropped owing to technical limitations) four valence electrons were distributed to form the CAS. The molecular orbitals were determined in a state-averaged CASSCF with the same weight for the ground and excited states. In the ICMRCI calculations, all single and double excitations from the CAS reference wave functions are taken into account [23, 24]. The molecular Hamiltonian was also augmented by a core–core repulsion correction (CCRC) in order to account for deviations from the point-charge repulsion between the Ca^{2+} cores. The CCRC was derived for internuclear distances of interest at the Hartree–Fock level with frozen atomic orbitals taken from a Ca^{2+} calculation using the ten-valence-electron pseudopotential adjusted to reference data from Wood–Boring (WB) scalar-relativistic all-electron calculations [PP(10)]. The present ICMRCI calculations were also corrected for size-consistency errors by means of the Davidson correction (Q). The basis set superposition error (BSSE), although of minor importance in the case of a large core pseudopotential approximation, was eliminated by means of the standard counterpoise method of Boys and Bernardi [25].

3 Results and discussion

The molecular calculations were performed for the Ca_2 dimer in the internuclear separation range from $3.25a_0$ to $50a_0$ with different step sizes. The calculations involve the ground state and low-lying excited states correlating up to the Ca $(4s4p)^1P$ term. The potential energies were evaluated with respect to the corresponding asymptotic energies taken at $R = 100a_0$. The potential curves for excited states are plotted relative to the corresponding experimental values of the atomic terms. Numerical values of the calculated potential energies are available from the authors (E.C.) upon request. The potential depths, D_e, and equilibrium positions, R_e, were derived using a cubic spline approximation to the calculated potentials around their equilibrium positions. On the other hand, the fundamental frequencies, ω_e were calculated by numerically solving the radial Schrödinger equation for nuclear motion with the corresponding potential. For this purpose the Numerov–Cooley method was applied.

3.1 Ground state

The $X^1\Sigma_g^+$ ground state of Ca_2 arises from two $(4s^2)^1S$ Ca atoms and is represented primarily by the single configuration wavefunction [core] $6\sigma_g^2 6\sigma_u^2$, where [core] represents the electronic configuration of the inner-shell electrons. The only possible long-range attractive force between two ground-state atoms is due to the dispersion

interaction caused by correlation between the fluctuating multipolar charge distributions of the atoms. In the region of intermediate internuclear separations where the molecule is formed, covalent bonding contributes substantially to the interaction energy. The calculated ICM-RCI dissociation energy of the Ca_2 ground state seemed to be somewhat overestimated ($D_e = 1170$ cm^{-1}, corrected for BSSE); therefore to improve the result, we recalculated the Ca_2 ground state by applying the CCSD(T) method. The CCSD(T) calculations were performed with two different Ca pseudopotentials; namely, we used the PP(2) pseudopotential and the Ne core ten-valence-electron pseudopotential adjusted to reference data from WB scalar-relativistic all-electron calculations [PP(10)]. In the latter case, we used the uncontracted (7s7p6d3f1g) basis set obtained as an extension of the Ca ecp10mwb basis set taken from the Molpro library. Both the pseudopotentials yield ground-state dissociation energies in close agreement with experiment; the PP(2) + CPP value is even a bit closer to the experimental data. Since a small-core pseudopotential calculation is usually thought to be the more accurate approach, the result obtained is probably due to an incomplete treatment of core–valence correlation with our PP(10) basis set. Finally, the CCSD(T) ground-state spectroscopic properties for Ca_2 are $D_e = 1035$ cm^{-1}, $R_e = 8.02a_0$ and $\omega_e = 62.4$ cm^{-1}, which agree quite well with the experimental values ($D_e = 1075 \pm 150$ cm^{-1}, $R_e = 8.09a_0$, $\omega_e = 64.9$ cm^{-1} [8] and $D_e = 1095 \pm 5$ cm^{-1}, $R_e = 8.08a_0$, $\omega_e = 65.07$ cm^{-1}) [12] determined from spectroscopic studies. On correcting for BSSE, the PP(10) potential is charcterized by $D_e = 1015$ cm^{-1} and $R = 8.25a_0$. The calculated $X^1\Sigma_g^+$ potential curve for Ca_2 is shown in Fig. 1. In addition, we extended our calculations on the ground state of Ca_2^+ for which, to the best of our knowledge, there exist no other theoretical data. In the calculations, we used the CCSD(T) scheme like in the case of Ca_2 by treating Ca_2^+ as a three-electron molecule. The calculated $X^2\Sigma_u^+$ potential curve is plotted in Fig. 2. The corresponding spectroscopic parameters extracted from the calculated potential energies are $D_e = 9817$ cm^{-1}, $R_e = 7.13a_0$ and $\omega_e = 132.3$ cm^{-1}.

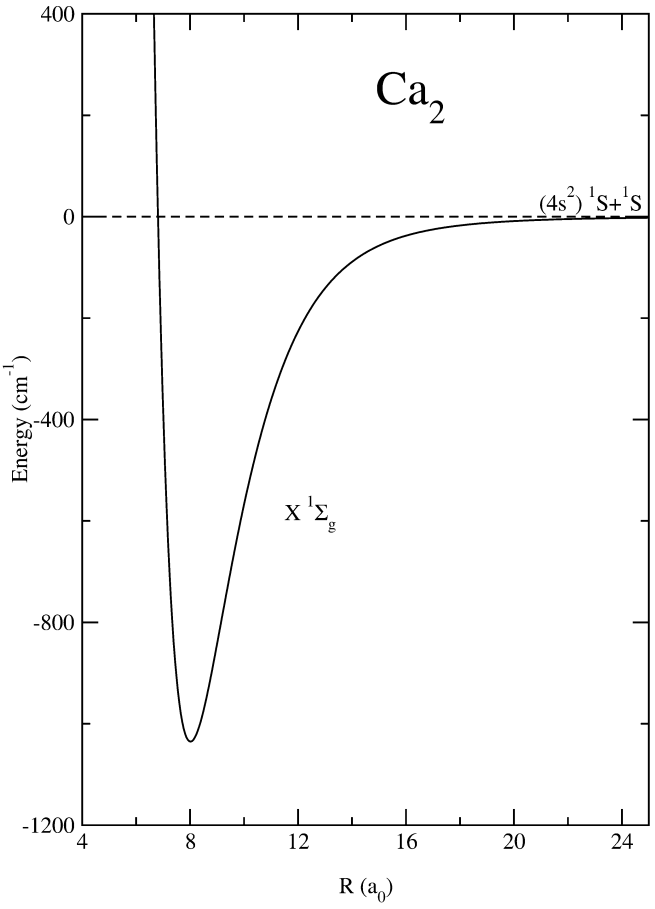

Fig. 1. Ground-state potential curve for the Ca_2 dimer

3.2 Excited states

The long-range part of the interaction of two like atoms in different energy states is dominated by the electrostatic dipole–dipole resonance energy. The leading term of the first-order dipole–dipole resonance energy is proportional to the $d_z^2 R^{-3}$ term, where d_z^2 is the square of the dipole transition moment between the ground state and the excited state of the atom [26]. The only experimentally known excited state of Ca_2 is $A^1\Sigma_u^+$. This state strongly couples with the ground state as a result of electric dipole transitions. Asymptotically, the $A^1\Sigma_u^+$ state is ascribed to the $^1P + {}^1S$ atomic limit and is represented by the $6\sigma_g^2 6\sigma_u 8\sigma_g$ and $6\sigma_g 6\sigma_u^2 8\sigma_u$ configurations and the long-range part of its interaction energy is dominated by the $-2d_z^2 R^{-3}$ term. Comparing the potential energy of the $A^1\Sigma_u^+$ state calculated at $R = 30a_0$ to its leading asymptotical term yields $d_z = 2.64$au, which agrees reasonably well with the ICMRCI value of 2.96au. The calculated bond strength of the $A^1\Sigma_u^+$ potential curve is 5810 cm^{-1} and agrees very well with the value of 5783 cm^{-1} derived from the laser-induced fluorescence data as quoted by Vidal [12]. Also the theoretical value of the electronic excitation energy between the minima of the X and A states, $T_e = 18979$ cm^{-1}, is in excellent agreement with the experimental value (18964 cm^{-1}) [12]. Absorption and emission bands attributed to Ca_2 have been observed by several groups, both in the gas phase and in matrix environments. Their definitive assignments to molecular transitions are still elusive. Experimentalists argue about whether the $A^1\Sigma_u$ state should be ascribed to the $(4p)^1P + {}^1S$ or $(3d)^1D + {}^1S$ asymptote [12, 14, 15]. The present calculations are believed to shed light on this question. The lowest-energy transition, appearing as a structured band at 15400 cm^{-1}, was observed first in gas-phase work by Sakurai and Broida [9], and was reinvestigated in more detail by Wyss [10]. Ultimately, this absorption band has been assigned to the $X^1\Sigma_g^+ \rightarrow (4p)^1\Sigma_u$ transition of Ca_2; this is not corroborated by the present investigation. In the light of our study, rather the Ca intercombination transition (15210 cm^{-1}) is responsible for this band ($X^1 0_g^+ \rightarrow A^3 0_u^+$ transition).

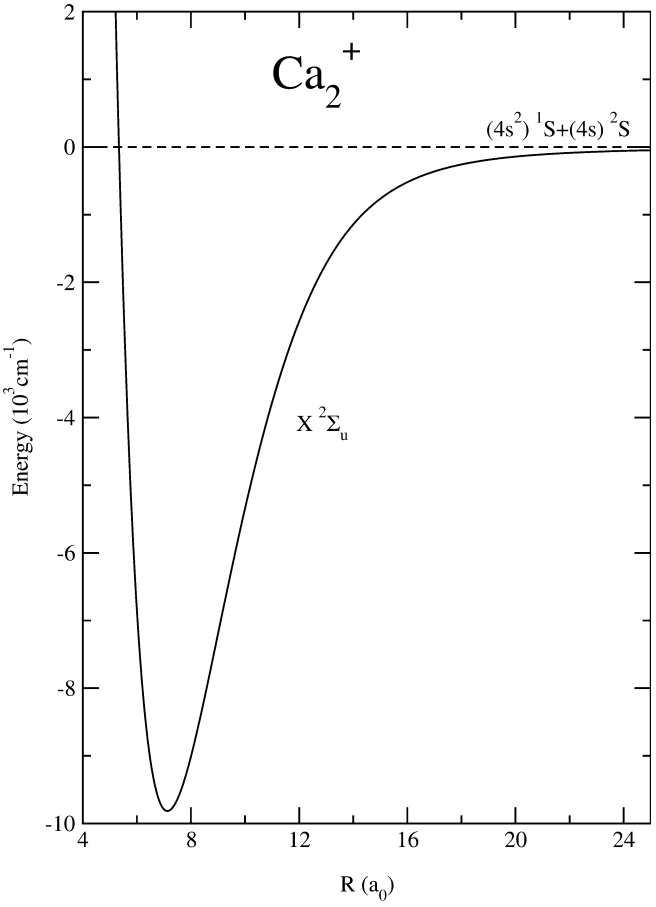

Fig. 2. Ground-state potential curve for Ca_2^+

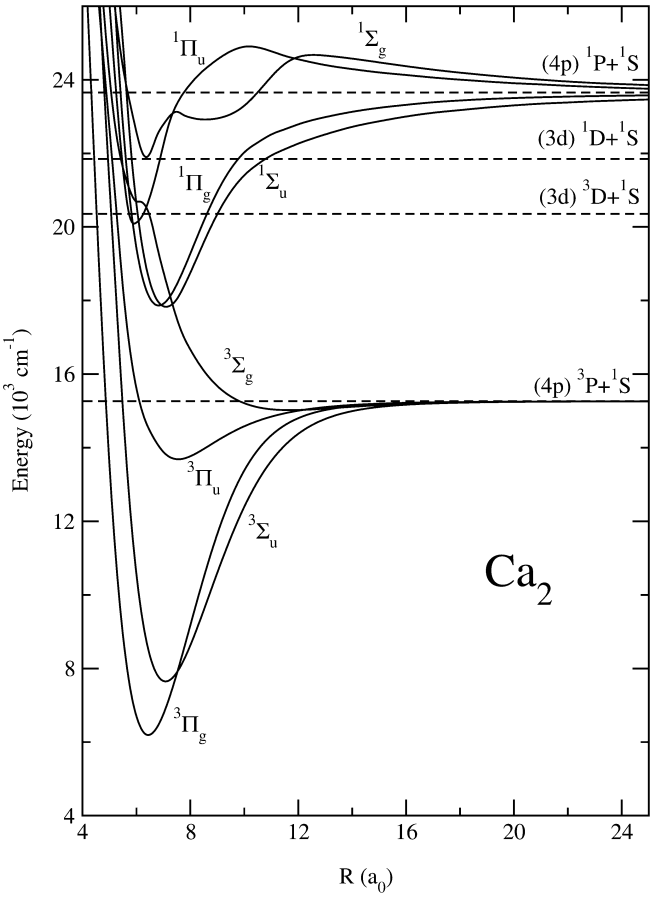

Fig. 3. Potential curves for the excited triplet and singlet states of the Ca_2 dimer correlating to the $^3P + {}^1S$ and $^1P + {}^1S$ asymptotes

Another excited state of Ca_2 which correlates with the Ca resonance level and strongly couples with the ground state is $^1\Pi_u$. The asymptotic configurations describing this state are $6\sigma_g 6\sigma_u^2 4\pi_u$ and $6\sigma_g^2 6\sigma_u 4\pi_g$. The long-range part of the interaction energy of the $^1\Pi_u$ state is dominated by $d_z^2 R^{-3}$. The $^1\Pi_u$ potential curve is shallower compared to that of $^1\Sigma_u$ and displays a potential barrier at about $R = 10a_0$ with declining repulsion towards larger internuclear separations. An analysis based on the calculated potential curves indicates that the $^1\Pi_u$ state can be responsible for the absorption spectrum of Ca_2 measured and analyzed first by Balfour and Whitlock [8] who observed 47 absorption bands in the region from 4800 to 5375 Å (20835–18605 cm^{-1}). This rovibrational spectrum was originally assigned to the $X^1\Sigma_g^+ \rightarrow (3d)^1D^1\Sigma_u$ transition, which cannot be confirmed by the present investigation. In turn, the $^1\Sigma_g^+$ state of Ca_2 converging to the same asymptote is defined at large distances by the $6\sigma_g 6\sigma_u^2 8\sigma_g$ and $6\sigma_g^2 6\sigma_u 8\sigma_u$ configurations. A simple molecular orbital analysis shows that this state should not be strongly bound, which has been also corroborated by the present calculations. Besides, the calculations show that this potential has a structure characterized by a potential barrier at about $R = 12a_0$ and is the result of the long-range dipole–dipole resonance interaction proportional to $2d_z^2 R^{-3}$ and a hump near $R = 7.5a_0$ (Fig. 3). In consequence, the potential curve possesses two minima owing to an avoided crossing with a higher state of the same symmetry, presumably arising from the $(4p)^3P + {}^3P$ asymptote not considered in this study. The last of the singlet states, $^1\Pi_g$, asymptotically described by the $6\sigma_g^2 6\sigma_u 4\pi_u$ and $6\sigma_g 6\sigma_u^2 4\pi_g$ configurations, has a potential depth comparable to that of $^1\Sigma_u$ but slightly shifted towards shorter internuclear separations. Here the long-range dipole–dipole resonance attraction is represented by the $-d_z^2 R^{-3}$ term. The spectroscopic parameters D_e and R_e of the states discussed are listed in Table 1. The most attractive triplet state of the Ca_2 dimer is $^3\Pi_g$, which is defined asymptotically by the same two configurations as $^1\Pi_g$ except for spin coupling. This state is metastable with respect to electric dipole transitions to the ground state and can serve as a molecular reservoir when used in laser applications. Another strongly bound triplet state of Ca_2 is $^3\Sigma_u^+$, described asymptotically by the same configurations as $^1\Sigma_u^+$. This state is the lowest-lying excimer state which can radiate to the ground state owing to SO mixing with the $^1\Pi_u$ state. In turn, the $^3\Pi_u$ state has a potential minimum of 1575 cm^{-1} at $R_e = 7.50a_0$. The most repulsive triplet state, $^3\Sigma_g^+$, has a shallow minimum of 240 cm^{-1} at $R_e = 11.50a_0$ and is almost flat at larger internuclear separations. In the range of shorter internuclear separations, this potential curve crosses the two higher singlet $^1\Sigma_u$ and $^1\Pi_g$ curves, which is of importance for the trap loss process of cold Ca atoms.

Potential-energy curves correlating to the $(3d)^1D + {}^1S$ asymptote are shown in Fig. 4. They are smooth with a well-defined unique minimum for each state. The corresponding D_e and R_e deduced from the calculated potential energies are listed in Table 1. Except for the two lowest states, $^1\Pi_g$ and $^1\Delta_u$, all the others have comparable binding energies in the range of internuclear separation 6–7a_0. As seen from Fig. 4, the triplet states, except for $^3\Sigma_g$, converging to the $(3d)^3D + {}^1S$ asymptote display roughly analogous behavior versus R as the singlet ones. The $^3\Sigma_g$ curve exhibits a hump at about $R = 6a_0$ due to repulsion with a higher-lying state of the same symmetry. It is worth noting that despite the multitude of states we found no avoided crossing for any pair of the calculated adiabatic potential curves. Surely, numerous avoided crossings would be induced by SO coupling not considered in this study. Nevertheless, the reported potential curves are suitable for some further applications. For example, they can be directly used in the calculations of the cross-sections for nonadiabatic transitions between the singlet and triplet states of Ca_2 as well as for collisionally induced intramultiplet transitions by applying quantum scattering methods in the close-coupling approach [17]. Simultaneously with the potential curves, also the dipole transition moments versus R between the ground state and the two excited $(4p)^1\Sigma_u$ and $(4p)^1\Pi_u$ dimer states were evaluated within the CASSCF approach. The calculated transition moments display a rather strong dependence on R in the range of short internuclear separations. This can prove to be of importance for the study of the radiative escape mechanism responsible for the trap loss rate in MOT experiments. The results obtained are presented in Fig. 5.

Table 1. Spectroscopic parameters $D_e(cm^{-1})$ and $R_e(a_0)$ for the excited states Ca_2

Singlet state	D_e	R_e	Triplet state	D_e	R_e
$(3d)\ ^1\Delta_g$	5330	7.25	$(4p)\ ^3\Sigma_g$	240	11.50
$(3d)\ ^1\Sigma_g$	5915	5.74	$(3d)\ ^3\Delta_g$	3080	7.48
$(4p)\ ^1\Sigma_g$	1682	6.25	$(3d)\ ^3\Sigma_g$	1450	7.75
$(3d)\ ^1\Pi_u$	6307	6.76	$(4p)\ ^3\Pi_u$	1575	7.50
$(4p)\ ^1\Pi_u$	3535	6.02	$(3d)\ ^3\Pi_u$	5732	6.76
$(3d)\ ^1\Sigma_u$	5290	6.74	$(4p)\ ^3\Sigma_u$	7604	7.00
$(3d)\ ^1\Delta_u$	9518	6.75	$(3d)\ ^3\Delta_u$	6186	6.52
$(4p)\ ^1\Sigma_u$	5810	7.02	$(3d)\ ^3\Sigma_u$	4620	6.74
$(3d)\ ^1\Pi_g$	15310	6.24	$(4p)\ ^3\Pi_g$	9062	6.52
$(4p)\ ^1\Pi_g$	5778	6.75	$(3d)\ ^3\Pi_g$	5270	6.75

The SO matrix elements calculated in this work were prompted by the recent studies of light-induced collisions of cold Ca atoms [16, 17]. SO coupling which mixes

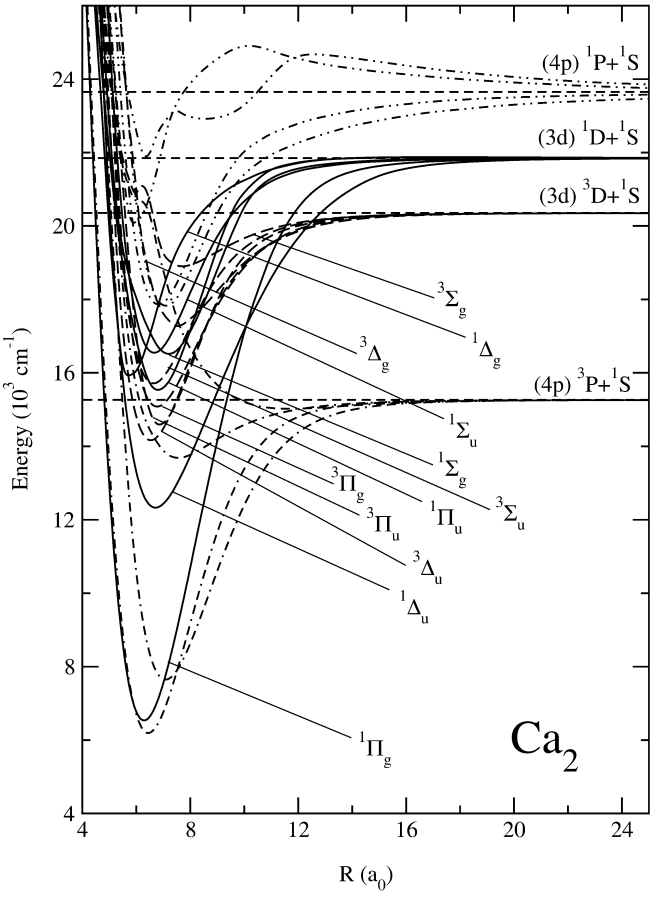

Fig. 4. Potential curves for the excited states of the Ca_2 dimer correlating to the $^3D + {}^1S$ and $^1D + {}^1S$ asymptotes. Potential curves arrising from the $^3P + {}^1S$ and $^1P + {}^1S$ asymptotes are also marked

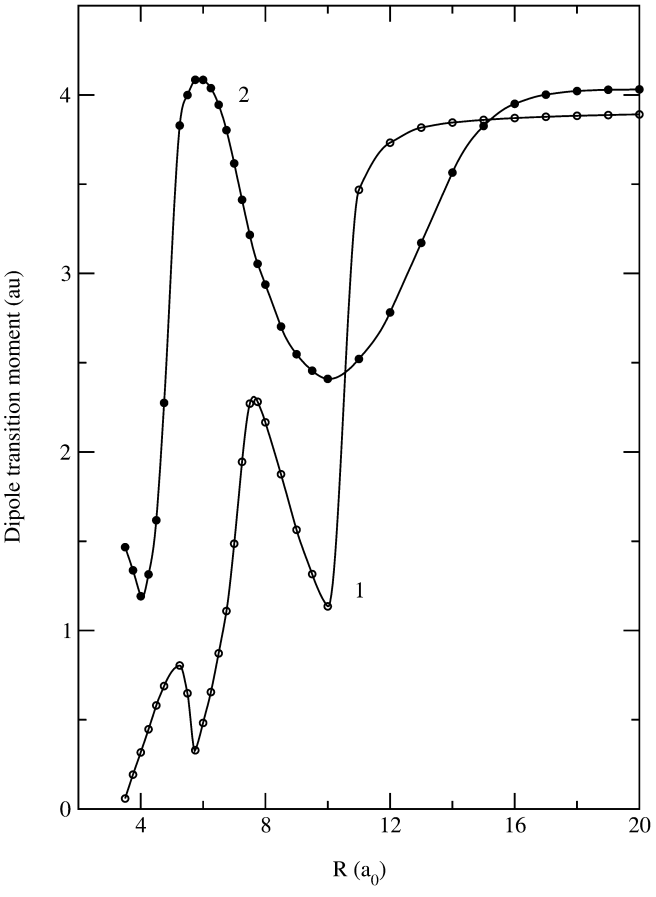

Fig. 5. Dipole transition moments between the ground state and the Ca $(4p)^1P$ state for the Ca_2 dimer as a function of R : $1\langle X^1\Sigma_g|x|(4p)^1\Pi_u\rangle$; $2\langle X^1\Sigma_g|z|(4p)^1\Sigma_u\rangle$

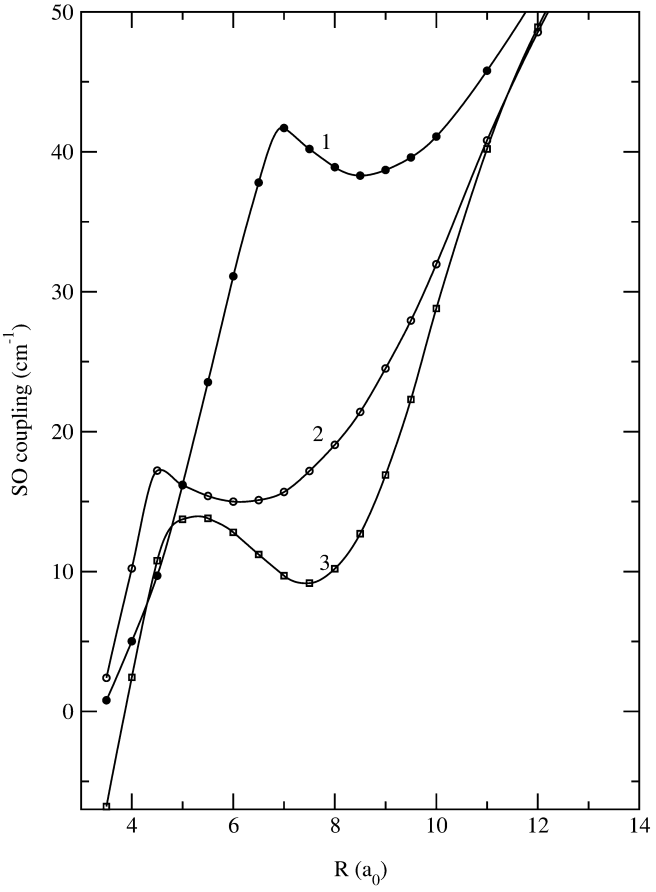

Fig. 6. Spin–orbit matrix elements for Ca_2 as a function of internuclear separation: $1\langle^3\Pi_g|\mathrm{SO}|^1\Pi_g\rangle$, $2\langle^3\Pi_u|\mathrm{SO}|^1\Sigma_u^+\rangle$, $3\langle^3\Sigma_g|\mathrm{SO}|^1\Pi_g\rangle$

the singlet and triplet states of an alkaline-earth dimer plays an important part in cold collisions. First of all, it is responsible for the fine-structure changing mechanism for trap loss rates observed in MOT experiments. Because its dependence on internuclear separation is unknown, it is usually assumed to be independent of R. Such an assumption is, of course, too simplified. Therefore evaluation of the SO coupling for Ca_2 versus R is of great importance. The corresponding SO matrix elements for Ca_2 as a function of R were calculated in the CASSCF approximation. They are presented diagrammatically in Fig. 6. Their numerical values are available upon request. As seen from the figure, the SO coupling for Ca_2 exhibits a rather strong dependence on R, particularly in the range of shorter internuclear separations. Asymptotically, all three matrix elements are equal to the corresponding atomic values, but with $R \to 0$ they decrease rapidly, taking values near zero. Moreover, all the matrix elements display a structure.

4 Conclusions

The low-lying valence states of the Ca_2 dimer have been studied by a combination of the CASSCF/ICMRCI and CCSD(T) methods. The calculated CCSD(T) ground-state potential curve for Ca_2 is reasonably consistent with the corresponding experimental data. In addition, the ICMRCI potential curve for the only experimentally known $A^1\Sigma_u$ state also agrees very well with experiment. The calculated SO coupling between the molecular states correlating with the $(4p)^1P$ and $(4p)^3P$ Ca states has proved to be strongly dependent on internuclear separation. Both the calculated SO coupling and the dipole $(4s^2)^1S$–$(4p)^1P$ transition moments are of great importance for better understanding of the trap loss mechanism in MOT experiments. The present results are also believed to be helpful in correct interpretation of the observed spectra arising from the Ca_2 dimer.

Acknowledgement. This work was supported by grant 5 P03B 082 21 from the Polish State Committee for Scientific Research (KBN).

References

1. Jones RO (1979) J Chem Phys 71: 1300
2. Stevens WJ, Krauss M (1977) J Chem Phys 67: 1977
3. Partridge H, Bauschlicher CW, Pettersson LGM, McLean AD, Liu B, Yoshimine M, Komornicki A (1990) J Chem Phys 92: 5377
4. Czuchaj E, Krośnicki M, Stoll H (2001) Theor Chem Acc 107: 27
5. Dyall KG, McLean AD (1992) J Chem Phys 97: 8424
6. Boutassetta N, Allouche AR, Aubert-Frecon M (1996) Phys Rev A 53: 3845
7. Allouche AR, Aubert-Frecon M, Nicolas G, Spiegelmann F (1995) Chem Phys 200: 63
8. Balfour WJ, Whitlock RF (1975) Can J Phys 53: 472
9. Sakurai K, Broida HP (1976) J Chem Phys 65: 1138
10. Wyss JC (1979) J Chem Phys 71: 2949
11. Miller JC, Mowery RL, Krausz ER, Jacobs SM, Kim HW, Schatz PN, Andrews L (1981) J Chem Phys 74: 6349
12. Vidal CR (1980) J Chem Phys 72: 1864
13. Vigue J (1981) J Phys Lett 42: L531
14. Hofmann RT, Harris DO (1984) J Chem Phys 81: 1047
15. Gondal MA, Khan MA, Rais MH (1995) Chem Phys Lett 243: 94
16. Zinner G, Binnewies T, Riehle F, Tiemann E (2000) Phys Rev Lett 85: 2292
17. Machholm M, Julienne PS, Suominen K-A (2002) Phys Rev A 65: 023401
18. Werner H-J, Knowles PJ, MOLPRO (a package of ab initio programs with contributions from Amos RD, Berning A, Cooper DL, Deegan MJO, Dobbyn AJ, Eckert F, Hampel C, Hetzer G, Leininger T, Lindh R, Lloyd AW, Meyer W, Mura ME, Nicklass A, Palmieri P, Peterson K, Pitzer R, Pulay P, Rauhut G, Schütz M, Stoll H, Stone AJ, Thorsteinsson T)
19. Müller W, Flesch J, Meyer J (1984) J Chem Phys 80: 3297
20. Fuentealba P, von Szentpaly L, Preuss H, Stoll H (1985) J Phys B 18: 1287
21. Czuchaj E, Krośnicki M, Stoll H (2000) Mol Phys 98: 419
22. Moore CE (1958) Atomic energy levels. NSRDS-NBS circular no. 467. US Government Printing Office, Washington, DC
23. Werner H-J, Knowles PJ (1988) J Chem Phys 89: 5803
24. Knowles PJ, Werner H-J (1988) Chem Phys Lett 145: 514
25. Boys SF, Bernardi F (1970) Mol Phys 19: 553
26. Hirschfelder JO, Meath WJ (1967) In: Hirschfelder JO (ed) Advances in chemical physics, vol 12. Wiley-Interscience, New York, pp 3–106